OPEN ACCESS

Evaluation of Brilaroxazine (RP5063) in a Bleomycin-Induced Rodent Model of Idiopathic Pulmonary Fibrosis

Laxminarayan Bhat [a]*, Seema R Bhat[a], Marie-Claude Nault[b], Marzena Biernat[b], Sebastien M. Labbe[b]

[a]Reviva Pharmaceutical Holdings, Inc., Cupertino, California, USA (19925 Stevens Creek Blvd Suite 100, Cupertino, CA 95014)
[b]IPS Therapeutique, Sherbrooke, Quebec, Canada (3035, Boul. Industriel, Sherbrooke, Québec J1L 2T9)

* Corresponding author: Lbhat@revivapharma.com

ABSTRACT
Idiopathic pulmonary fibrosis pathology involves serotonin (5-HT), with an increased expression of $5\text{-HT}_{2A/2B/7}$ receptors in the lungs. This study tests the hypothesis that brilaroxazine (RP5063), an agent with a potent binding affinity for serotonin $5\text{-HT}_{1A/2A/2B/7}$ and dopamine $D_{2/3/4}$ receptors, and moderate affinity for the 5-HT transporter, dosed at 15 mg twice daily (b.i.d.) shows efficacy as compared with placebo in a bleomycin (BLM)-induced model using Sprague Dawley rats.
On Day 0, four groups received BLM-induction, and one received placebo. On Day 1, one group started on brilaroxazine (BT). On Day 10, two groups started on brilaroxazine (BI) and one continued on the vehicle (BLM). All interventions continued until Day 20.
Compared with BLM, BT and BI sustained survival at 90.5% and 89.5%, respectively ($P<0.05$) and maintained weight ($P<0.01$). BT normalized pulse pressure and cardiac output. It also lowered respiratory resistance, hydroxyproline, lung weight, bronchoalveolar lavage fluid cell counts, and total protein ($P<0.05$). BI decreased hydroxyproline and reduced cell counts ($P<0.01$). Brilaroxazine lowered Ashcroft scores and Masson's Trichome staining ($P<0.001$) to grade fibrosis and assess collagen deposition, respectively. Both brilaroxazine groups reduced proinflammatory and fibrotic cytokines ($P<0.05$).
Brilaroxazine attenuated BLM-induced pulmonary fibrosis, inflammation, and extracellular deposition and improved cardiac and pulmonary functions in rodents.

Keywords: Anti-inflammatory, Anti-fibrotic, Brilaroxazine, Bleomycin-induced rat model, Idiopathic pulmonary fibrosis, Interstitial lung disease

Introduction

Idiopathic pulmonary fibrosis (IPF) is a chronic, progressive, and debilitating lung disease[1]. This condition presents with a global prevalence of ~3 million, a median survival time of two to five years, and 50,000 deaths annually in the U.S.[1–6].

IPF involves chronic inflammation and progressive fibrosis of the alveoli[7]. This pathology leads to destroyed lung architecture, reduced lung capacity, impaired oxygenation, and a decline in lung function[3,7,8].

Treatment involves either early referral for lung transplantation, palliative care, and clinical trials[9,10]. Various interventions, including commonly used agents (e.g., corticosteroids and immuno-suppressants), are limited and not supported in current guidelines[9,11,12]. Two Food and Drug Administration (FDA) approved treatments – Nintedanib (Ofev®), and Pirfenidone (Esbriet®) – are inadequate in improving functional decline and disease progression[13,14]. Hence, survival continues as an unmet need[11].

Various studies have implicated serotonin (5-hydroxytryptamine; 5-HT) in the pathophysiology of IPF. It exerts both a vasoactive effect on pulmonary arteries and stimulation of lung myofibroblast actions[4,15]. Pulmonary 5-HT appears to mediate effects through $5\text{-HT}_{2A/2B/7}$ receptors[16–18]. Terguride (a $5\text{-HT}_{2A/2B}$ antagonist), SB215505 (5-HT_{2B} receptor antagonist), and SB269970 (a 5-HT_7 receptor antagonist) were observed to attenuate the bleomycin-induced pulmonary fibrosis in rodents[19–21].

Brilaroxazine (RP5063), a multimodal modulator of dopamine (D) and 5-HT receptors, is a promising new agent[22,23]. It displays a high affinity for $D_{2/3/4}$ and $5\text{-HT}_{2A/2B/7}$ receptors and moderate affinity for the serotonin transporter (SERT or 5-HTT)[23,24]. Brilaroxazine brings an established phase 1 and phase 2 efficacy, safety, and pharmacokinetic profile based in healthy volunteers and schizophrenia patients[23,25,26]. Its effects on vascular fibrosis (5-HT_{2B} receptor), proliferation ($5\text{-H}_{2A/2B}$ receptor), relaxation (5-HT_{2A} receptor), and inflammation (5-HT_7 receptor) have created interest in brilaroxazine as a treatment option[22,27,28]. This study was undertaken to build on the pulmonary arterial hypertension (PAH) preclinical experience[22,27,28]. It was designed to assess whether brilaroxazine dosed at 15 mg twice-daily produces greater efficacy, as compared with placebo, in a bleomycin (BLM)-induced rat model.

Materials and Methods
Study Animals
The investigation involved 34 male Sprague Dawley rats (weights: 275-300 g; ages: 8 weeks; Charles River Laboratories, St. Constant, Quebec, Canada) were randomized for equal distribution according to their body weight into four groups. The study schedule was such that an equal number of animals per treatment group were monitored and processed on each harvest day (when possible).

The institutional animal ethics committee of IPS Therapeutique (IPST) approved the study by the principles of the Canadian Council on Animal Care (CCAC). IPST identified, housed, and cared for the animals per the CCAC guidelines.

Study Design
The objective of this parallel-design study was to evaluate the effectiveness of brilaroxazine started on Day 1 and Day 10 following BLM-induction on the functional, histologic, and pathophysiological parameters in the BLM-induced model[29,30].

Study Methods
On Day 0, animals in Group 1 (Sham; N=5) received one intratracheal administration of the vehicle, 0.250 mL of vehicle 0.9% saline solution (Fig. 1). Animals in Groups 2 to 4 (n=9, 10, 10, respectively) received a single intratracheal instillation of 0.250 mL (5 U/kg – 3.33 mg/kg) of bleomycin sulfate (# 9041-93-4, Cayman Chemicals, Ann Arbor, MI, USA) solution. From Day 1 to 10, investigators administered the vehicle to Groups 1, 2, and 4. Brilaroxazine 15 mg/kg per gavage twice daily (b.i.d.) was administered to Group 3 as treatment from Day 1 to 20 (Group 3, BT). The investigators continued administration of the vehicle to Group 1 (Sham) and Group 2 (BLM) until Day 20. From Day 10 to 20, the Group 4 received 15 mg/kg per gavage twice-daily (b.i.d.) brilaroxazine as an intervention treatment (Group 4, BI). During the treatment period, food and water were provided *ad libitum* to the rats. On each day, the investigators monitored animals for behavior, general health status, and survival. Body weight and food intake were also measured.

For brilaroxazine, the 15 mg/kg b.i.d. dose was chosen based on data from the PAH preclinical experience (Bhat et al., 2017[b]). The solution used was prepared by dissolving 750 mg of brilaroxazine in 500 mL of sterile 5% glucose solution to obtain a solution of 1.5 mg/mL. For bleomycin, 50 mg of drug was weighed and dissolved in 12.5 mL of sterile 0.9% Saline solution was added to obtain a solution of 4 mg/mL. The vehicle was created by dissolving 50 g of glucose in 1 L of water to result in a 5% solution.

Fig. 1 Schedule of various treatments of the animals during the bleomycin-induced IPF study
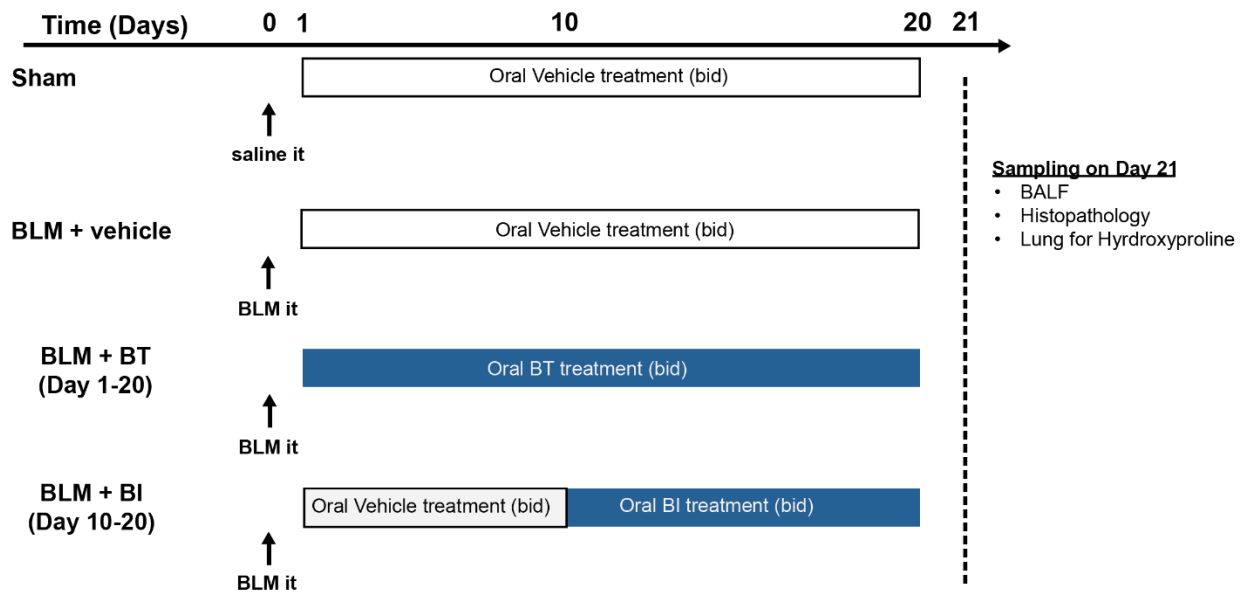
BALF: Bronchoalveolar lavage; BLM: Bleomycin; Sham: Non-induced animals with the vehicle.
BT: Brilaroxazine treatment Days 1-20; BI: Brilaroxazine treatment Days 10-20.

On Day 21, animals were anesthetized (Isoflurane, 2% 1.5L/min) and instrumented. Hemodynamic parameters (systemic arterial blood pressure, heart rate, and oxygen saturation) were recorded continuously for at least 5 minutes. At the end of the recording, the investigators collected blood samples. After the investigators, exsanguinated the animals, they flushed the pulmonary circulation with 0.9% NaCl, and tissues (lungs, trachea, and heart) were harvested altogether from the thoracic cavity for further analysis.

Parameters Measured on Surgery Day
Cardiac activity was recorded continuously during the surgical procedure. Cardiac activity was monitored using three electrocardiographic (ECG) contact electrodes (Harvard BioSciences Inc., Holliston, MA) placed in a lead-I/II configuration and connected to an IsoDam8 differential amplifier (World Precision Instruments, LLC, Sarasota, FL). Heart rate (HR) was recorded using duplicate systems: from the ECG records (RR-intervals) and using an N-595 pulse oximeter (Nellcor, Plymouth, MN) attached to the left front paw of the animal. The heart rate values derived from the pulse oximeter were measured in beat per minutes (bpm) using cursor readings in Clampfit 10.2.0.14 (Axon Instrument Inc., Foster City, California, USA, [now Molecular Devices Inc.]). Blood oxygen saturation (SpO$_2$) was measured using a pulse oximeter signal attached to the left front paw of the animal. Saturation values were measured in percentages

using cursor readings in Clampfit 10.2.014.
Systemic arterial blood pressure (SAP) was monitored continuously using an intra-arterial fluid-filled catheter connected to a pressure transducer (AD Instruments, Colorado Springs, CO), with diastolic and systolic pressures values measured in mm Hg using Clampfit 10.2.0.14. Calculation of mean SAP (mSAP) and pulse pressure (PP) used the following formulas: 1— mSAP = diastolic systemic pressure + ([systolic systemic pressure − diastolic systemic pressure] / 3); and 2— PP = systolic systemic pressure − diastolic systemic pressure. Investigators calculated pulse pressure as the difference between systolic and diastolic readings. After being harvested, the investigators connected the trachea to the cannula of a perfusion system. The investigators then clamped left lung while they injected 5 mL of cold phosphate-buffered-saline (PBS) solution into the trachea to perform bronchoalveolar lavage to obtain fluid (bronchoalveolar lavage fluid, BALF) of the right lobe of the lungs for further analysis (Total cell counts and cytokines measurement). Once the investigators collected the BALF sample, it was centrifuged at 1200 rpm for 10 minutes at 4°C. They froze the supernatant at -80°C until cytokines analysis. The cells were then resuspended in PBS and counted with a hemocytometer.
Investigators expressed organ weights as relative percentages and calculated as follows: Relative organ weight = (organ weight × 100) / body weight.

Histological Preparation and Categorization

For each rat, the left lobe of the lungs was harvested, perfused and fixed with 10% neutral buffered formalin. A transversal section of the middle left lobe was cut and forwarded in 10% neutral buffered formalin (NBF) solution to the Institute for Research in Immunology and Cancer (Montreal, Quebec, Canada). Tissues were embedded, sliced (5-µm thickness), mounted, and conventionally stained. Staining included hematoxylin and eosin (H&E) and Ashcroft score and finally, a Masson's trichrome staining for the fibrosis quantification. Glass slides containing fixed and stained tissues were visualized at 20 × magnification (Eclipse T100 microscope, Nikon, Melville, NY). The investigators selected at least five non-overlapping view fields/lung for microphotographs (Nikon DS-Fi1 digital camera with Nikon NIS Elements 4.30, Nikon, and Melville, NY).

Alveolar septa and lung structure were estimated using the H&E slides. Tissue was scored with a modified Ashcroft Scale accordingly to the means of the five non-overlapping view fields previously selected. These included the following ratings: (1) 0: No fibrotic changes in alveolar septa, normal lungs; (2) 1: Isolated gentle fibrotic changes, alveoli partly bigger and rarefied (less than 3x), no present of fibrotic masses; (3) 2: Clearly thicker alveolar septa (more than three times) with knot-like formation but not connected to each other, alveoli partly larger and rarefied, no present of fibrotic masses; (4) 3: Contiguous fibrotic walls in whole microscopic field, alveoli partiallylargers and rarefied, no presence of fibrotic masses; (5) 4: Variable alveolar septa, single fibrotic masses (less than 10% of microscopic field); (6) 5: Variable alveolar septa, confluent fibrotic masses (between 10% and 50% of microscopic field), lung structure severely damaged but still preserved; (7) 6: Variable, mostly not existent alveolar septa, large contiguous fibrotic masses (more than 50% of microscopic field), lung architecture mostly not preserved; (8) 7: non-existent alveolar septa, alveoli nearly obliterated with fibrous masses but still up to five air bubbles; and (9) 8: non-existent alveolar septa, complete obliteration with fibrotic masses.

Glass slide tissue stained with Masson's Trichrome was also visualized using a scanner to determine the percentage of the fibrotic tissue on the slice. The investigators performed analysis with specific software (ImageJ v1.48, NIH). For each captured image, the investigators determined the collagen fraction as the ratio of the collagen surface area concerning the total lung surface.

Hydroxyproline Determination

Hydroxyproline content was determined using a colorimetric assay kit (STA-675, Cell Biolabs Inc, CA, USA). Part of the right lobe was removed and homogenized in 0.1 mL of water. The investigators treated the homogenate within 0.1 mL of 10 N hydrochloric acid (HCl) for 6 hours at 120°C. Following the addition of 5 mg of activated charcoal, the investigators centrifuged the samples at 10,000 revolutions per minute (rpm) for five minutes, and the supernatant was transferred to a new tube and processed according to the assay's instructions. They measured absorbance at 540 nm, and the amount of hydroxyproline was determined and corrected for protein content.

Cytokine Quantification

On Day 21, the investigators collected BALF samples immediately following their exsanguination of the animal. For all groups, the investigators saved one-half of each sample for analysis of the following cytokines: (1) Macrophage inflammatory protein 1 (MIP1); (2) Monocyte chemoattractant protein 1 (MCP1); (3) Interleukin (IL)-6; (4) Interferon gamma-induced protein 10 (IP10); and (5) RANTES. The cytokine analysis was performed using a Luminex assay (Eve Technologies, Calgary, Alberta).

Analysis and Statistics

The primary outcomes involved survival and weight. Additional parameters of note included cardiopulmonary and pressure parameters at surgery, tissue weights, histologic samples, bronchoalveolar pulmonary lavage fluid cell counts, hydroxyproline levels, and cytokine. Results are expressed as means $\pm$ the standard error of the mean (SEM). Comparisons were made on normally distributed data using analysis of variance (ANOVA), followed by a Fisher post hoc test to assess the difference between BLM group with Graph Pad Prism Software version 7.0 for MacIntosh (San Diego, CA, USA). Comparisons included Sham versus BLM and treatment(s) versus BLM. The investigators did not evaluate treatment differences. Differences were statistically significant when P values were less than 0.05.

Results

Animal Survival and Weights

Of the 19 animals in Groups 2 and 4, the survival rate at Day 10 was 82% during this period ($P<.05$, Sham). In contrast, the survival rate in non-induced (Group 1) was 100% ($P<.05$, BLM) (Fig. 2A). At Day 21, the survival rate for the BLM (Group 2)

dropped to 62% (*P*<.05, Sham), whereas BT and BI survival rates were 90% and 89.5% (*P*<.05, BLM), respectively (Fig. 2B). Animals in the Sham group continued at 100%. Mirroring the survival rates were those of body weight (Fig. 2C). Three weeks after BLM induction, the body weight of those in the Sham group increased by approximately 50%; however, the rats in the BLM group was significantly lower (*P*<0.05, Sham). BT significantly alleviated BLM-induced weight loss by Day 21 (*P*<0.01, BLM), as compared with the BLM group. BI administered from Day 10 following the BLM induction, slightly increased body weight, as compared to BLM-treated rats at Day 21.

Fig. 2 Survival curves from Day 1-10 (A) and Day 11-21 (B), and body weights (C) of Sham, BLM-induced, treatment group animals
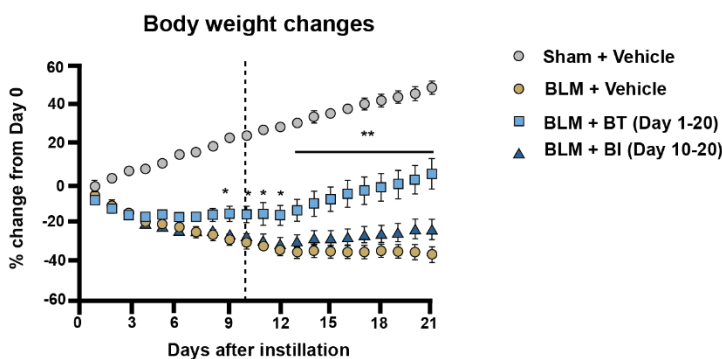
A.
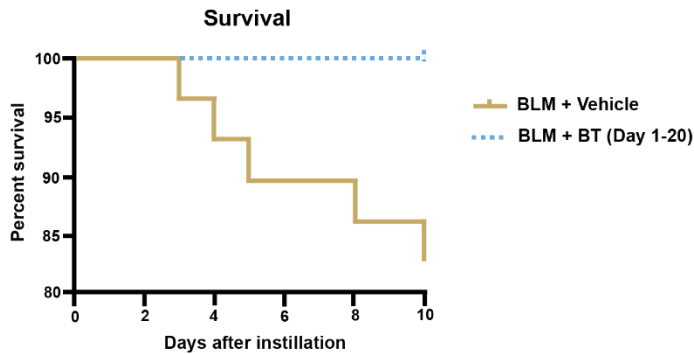
B.
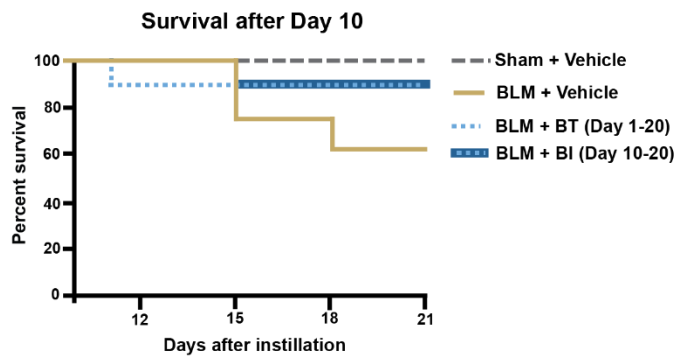
BALF: Bronchoalveolar lavage
BLM: Bleomycin
Sham: Non-induced animals with the vehicle
BT: Brilaroxazine treatment Days 1-20BI: Brilaroxazine treatment Days 10-20
*P<0.05 BLM+Veh; as compared to Sham
P<0.05; as compared to BLM+Veh.

C.

Hemodynamic and Cardiac Effects

Hemodynamic parameters were recorded on Day 21 (Fig. 3). Animals in the BLM experienced a significant effect (*P*<0.05, Sham) of the arterial pulse pressure (Fig. 3A) and cardiac output (Fig. 3C). Ventricular dysfunction (insufficient left ventricular preload) and hypovolemia might account for these observations with pulse pressure.

Animals in the BT experienced an improved arterial pulse pressure (*P*<0.05, BLM), and were at a similar level that was experienced by those in the Sham group.

Additionally, animals in both brilaroxazine groups had restored cardiac output, with BT significant as compared with those on BLM ($P<0.01$). BI slightly restored the arterial pulse pressure and cardiac output; these effects were not significant (NS) as a result due to the small sample size and short period of intervention. As compared with the non-BLM group, BT showed high cardiac output (NS) and BI displayed a lower effect (NS).

Heart rate was relatively similar in all groups (Fig. 3B).

Concerning the systemic arterial pressure (Fig. 3 D-F), while the investigators noted no differences among the groups, they did observe that animals in the BLM group displayed a non-significant reduction (~29%) of systemic arterial pressure; this effect was probably a consequence of the cardiac output reduction.

Fig 3. Hemodynamic and cardiac parameters (A-C) and systemic arterial pressures (D-F) measured on Day 21
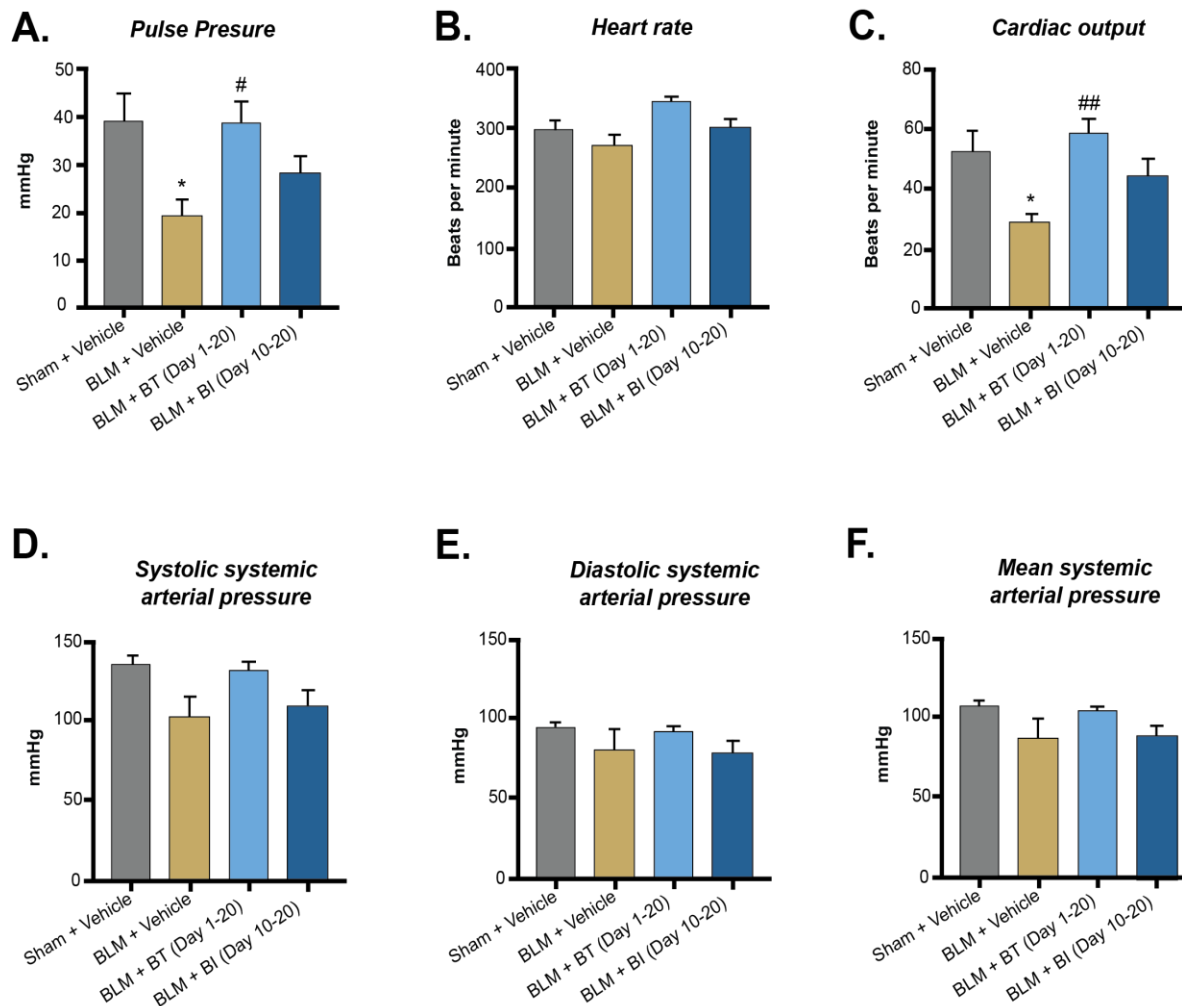
BALF: Bronchoalveolar lavage; BLM: Bleomycin; Sham: Non-induced animals with the vehicle.
BT: Brilaroxazine treatment Days 1-20; BI: Brilaroxazine treatment Days 10-20.
*$P<0.05$ BLM+Veh; as compared to Sham.
$P<0.05$; as compared to BLM+Veh.

### Parameters Reflective of Pulmonary Fibrosis and Function

Pulmonary fibrosis is known to induce respiratory resistance; resistance to the air flow through the respiratory tract during inhalation and exhalation. This resistance reduces gas exchange (oxygen-carbon dioxide [O_2-CO_2]) in the alveolar and

contributes to reducing lifespan. The BLM animals showed a significant ($P<0.001$, Sham) increase in respiratory resistance (Figure 4A). Animals in the BT group displayed a significant reduction in this parameter ($P<0.05$, BLM), while those in the BI group showed improvement ($P=0.10$, BLM); however, this effect was not statistically significant.

The hydroxyproline content in the lung was also measured to evaluate the presence of pulmonary fibrosis (Fig. 4B) and reflected changes seen in respiratory resistance. The BLM animals displayed a two-fold higher hydroxyproline concentration ($P<0.05$, Sham). Those in the BT ($P<0.05$, BLM) and BI ($P<0.01$, BLM) groups had a significant diminution in hydroxyproline concentration.

Fig. 4. Respiratory resistance (A) lung hydroxyproline (B) measured on Day 21
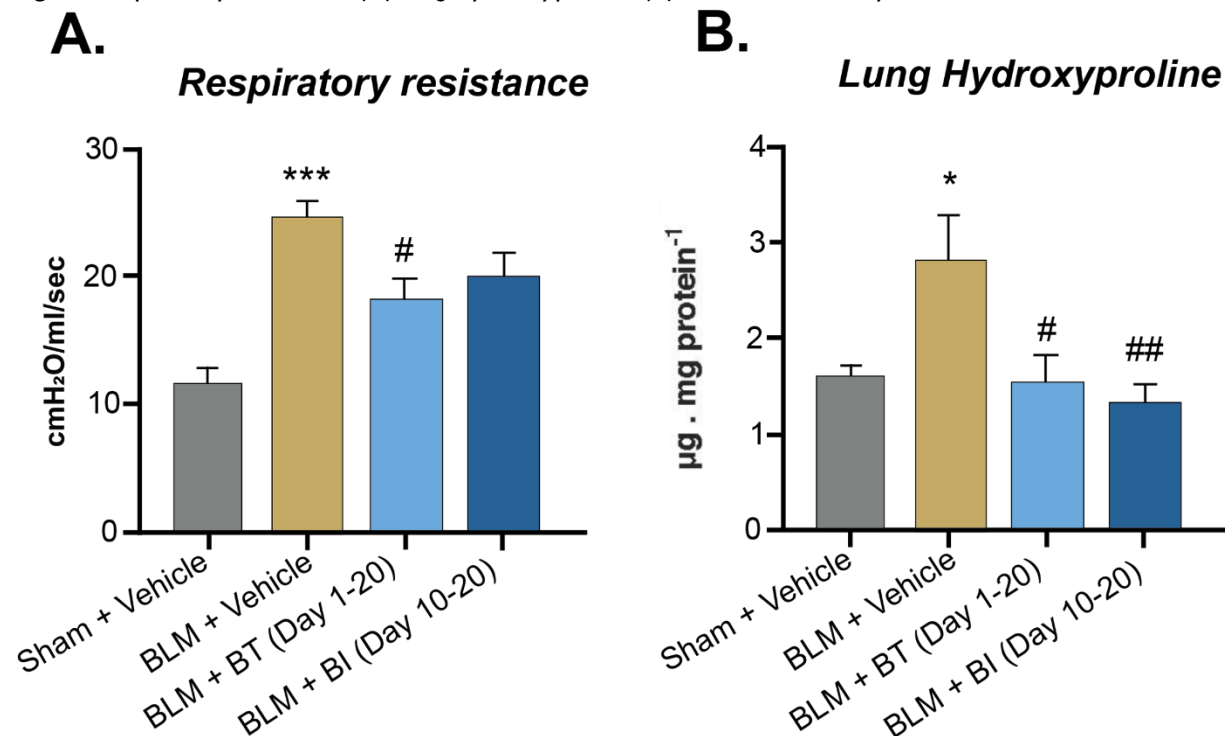
A.
Respiratory resistance

B.
Lung Hydroxyproline

BALF: Bronchoalveolar lavage; BLM: Bleomycin; Sham: Non-induced animals with the vehicle.
BT: Brilaroxazine treatment Days 1-20; BI: Brilaroxazine treatment Days 10-20.
*$P<0.05$ BLM+Veh; as compared to Sham.
*** $P<0.001$; as compared to Sham.
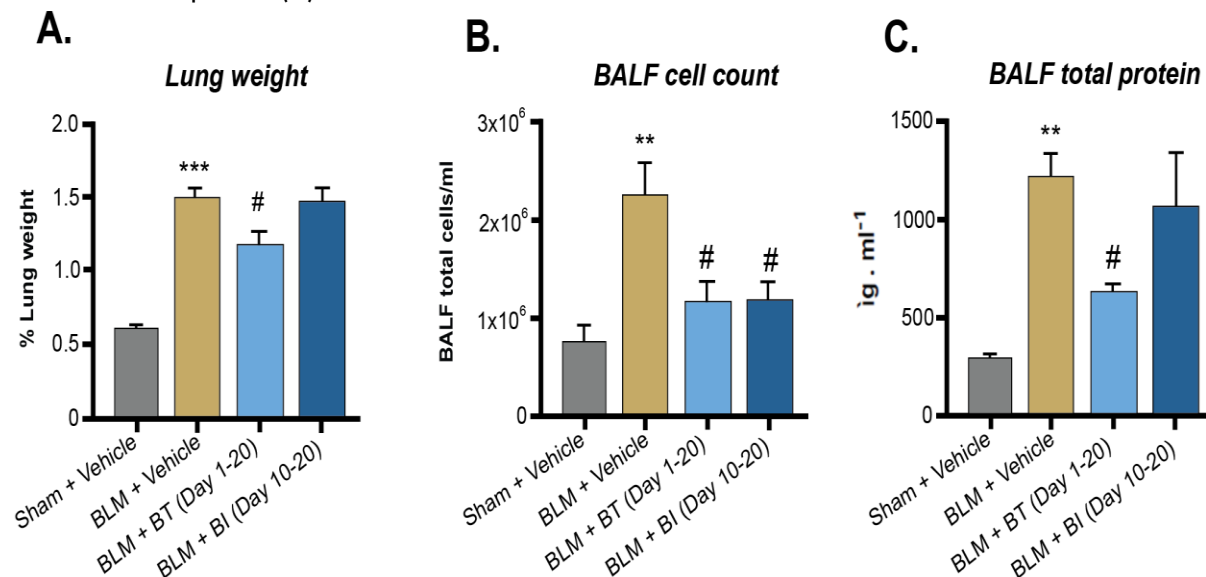# $P<0.05$; as compared to BLM+Veh.
$P<0.01$; as compared to BLM+Veh.

Reflective of the pulmonary changes induced by BLM, animals in the BLM group had significantly ($P<0.01$, Sham) higher lung weights (Fig. 5A), suggesting the presence of edema. Lung weight of the BT animal was significantly lower ($P<0.05$, BLM). The lung weight decreases in the BI group were only numerical.

Total cell count (inflammation, Fig. 5B) and total protein content (edema, Fib. 5C) were obtained from BALF of the right lobe of the lungs to reinforce lung weight measurements and reflect the presence of pulmonary edema. Both cell counts and protein levels in the BLM animals showed a significant increase ($P<0.01$, Sham). Animals in the BT group showed a reversal in both cell counts and protein levels (both, $P<0.05$, BLM). Animals in the BI group significantly reduced the total cell counts ($P<0.05$, BLM); however, they showed only numerical improvement reduction of BALF protein concentration. Staining of lung tissue provided additional evidence reflective of the development of pulmonary fibrosis with BLM and attenuation with brilaroxazine treatment. As reflected in H&E staining (Fig. 6), the Ashcroft Score in the BLM group lung tissue samples (Fig. 6 A, C) was significant ($P<0.001$, Sham). Of the treatments, only samples obtained from BT animals displayed a significant reduction in these lung parenchymal fibrotic changes (Fig. 6C), ($P<0.001$, BLM).

Pulmonary fibrosis is characterized by excessive collagen disposition in the lung, as reflected by percent fibrosis areas measured with Masson's trichrome staining. Staining samples from animals in the BLM showed a significant ($P<0.001$, Sham) increase in the percentage of fibrosis disposition in the lung on Day 21 (Fig. 6 B, D). Therapeutic intervention with brilaroxazine (BT) significantly reduced these changes ($P<0.001$, BLM). These results correlate nicely with the previously presented hydroxyproline concentration quantification.

Fig. 5. Parameters reflective of pulmonary edema at Day 21 including lung weight (A), BALF cell count (B), and BALF total protein (C)

BALF: Bronchoalveolar lavage; BLM: Bleomycin; Sham: Non-induced animals with the vehicle.
BT: Brilaroxazine treatment Days 1-20; BI: Brilaroxazine treatment Days 10-20.
**$P<0.01$ BLM+Veh; as compared to Sham.
*** $P<0.001$; as compared to Sham.
# $P<0.05$; as compared to BLM+Veh.

Investigators measured reflective of BLM-induced effects on cardiopulmonary capacity, blood oxygen saturation (Fig. 7A) and blood lactate levels (Fig. 7B) at Day 21. The BLM animals showed a significant decrease in saturation and a significant increase in blood lactate levels (both; $P<0.01$, Sham). Animals in the BT group showed normalization of the blood oxygen levels ($P<0.05$, BLM). The saturation levels in BI animals improved and were numerically better than those the BLM group. While the treatments induced a diminution of blood lactate levels, both the BT and BI were significant ($P<0.01$, $P<0.05$, respectively, versus BLM).

BLM-Induced Inflammatory and Fibrogenic Cytokines
To evaluate the impact of treatment on BLM-induced inflammatory and fibrogenic cytokines, the analysis of BALF from Day 21 quantified levels of MIP1, MCP1, IL-6, IP10, and RANTES (Fig. 8A-E). Animals in the BLM group displayed a significant increase in all the five cytokines levels ($P<0.05$ for MIP1 and MCP1; $P<0.01$ for IP10 and RANTES, Sham). None of the treatments statistically reversed the production of MIP-1 (Fig. 8A), though BT slightly reduced the production of this cytokine. While the brilaroxazine treated animals showed reductions in MCP-1 concentrations (Fig. 8B), only those in the BT group showed a significant decrease ($P<0.05$, BLM). Animals in both treatment groups had numerically (BT, BI) reduced IL6 levels (Fig. 8C) Animals in

both BT and BI groups showed significant reductions in IP10 (Fig. 8D) ($P<0.01$, BLM). Finally, animals in both brilaroxazine treated animals had significantly reduced RANTES cytokine levels (Fig. 8E) ($P<0.01$, BLM).

Discussion
***Relationship of the Underlying IPF Pathology and the Effect of Brilaroxine***
This study was the first preclinical evaluation in animals of the effects of brilaroxazine in the IPF setting. It evaluated both the impact on mortality and cardiorespiratory function and critical pathologic processes including inflammation and fibrosis. Such design and endpoints were consistent with the standards for BLM-induced IPF models[29,30]
Chronic inflammation is a contributing factor in the development of pulmonary fibrosis. The infiltration of inflammatory cells (e.g., macrophages, lymphocytes, and neutrophils) drive the differentiation of fibroblasts to myofibroblasts, which secretes collagen and other extracellular materials into the alveolar interstitial space to produce pulmonary fibrosis.
Accordingly, this study assessed the effects of brilaroxazine on BLM-induced pulmonary inflammation and fibrosis development. Previous animal studies in PAH demonstrated that brilaroxazine inhibited monocrotaline- or Sugen 5416-hypoxia-induced inflammation due to decreased cytokine and

chemokine levels, respectively, in the lung tissue[22,27]. BLM-induction in this study resulted in a three-fold increase in the total number of cells in BALF, an increase in BALF protein, and lung weight. Both brilaroxazine treatment strategies decreased the BLM-induced rise of BALF cells by approximately 46%. Brilaroxazine, particularly BT, reduced pulmonary edema, as evidenced by the reduction in BALF protein content and the lower relative lung weight.

Fig. 6. Morphology changes displayed by H&E staining and Ashcroft Score (A, C) and collagen deposition and Masson's trichrome staining (B, D) induced by BLM in rats on Day 21
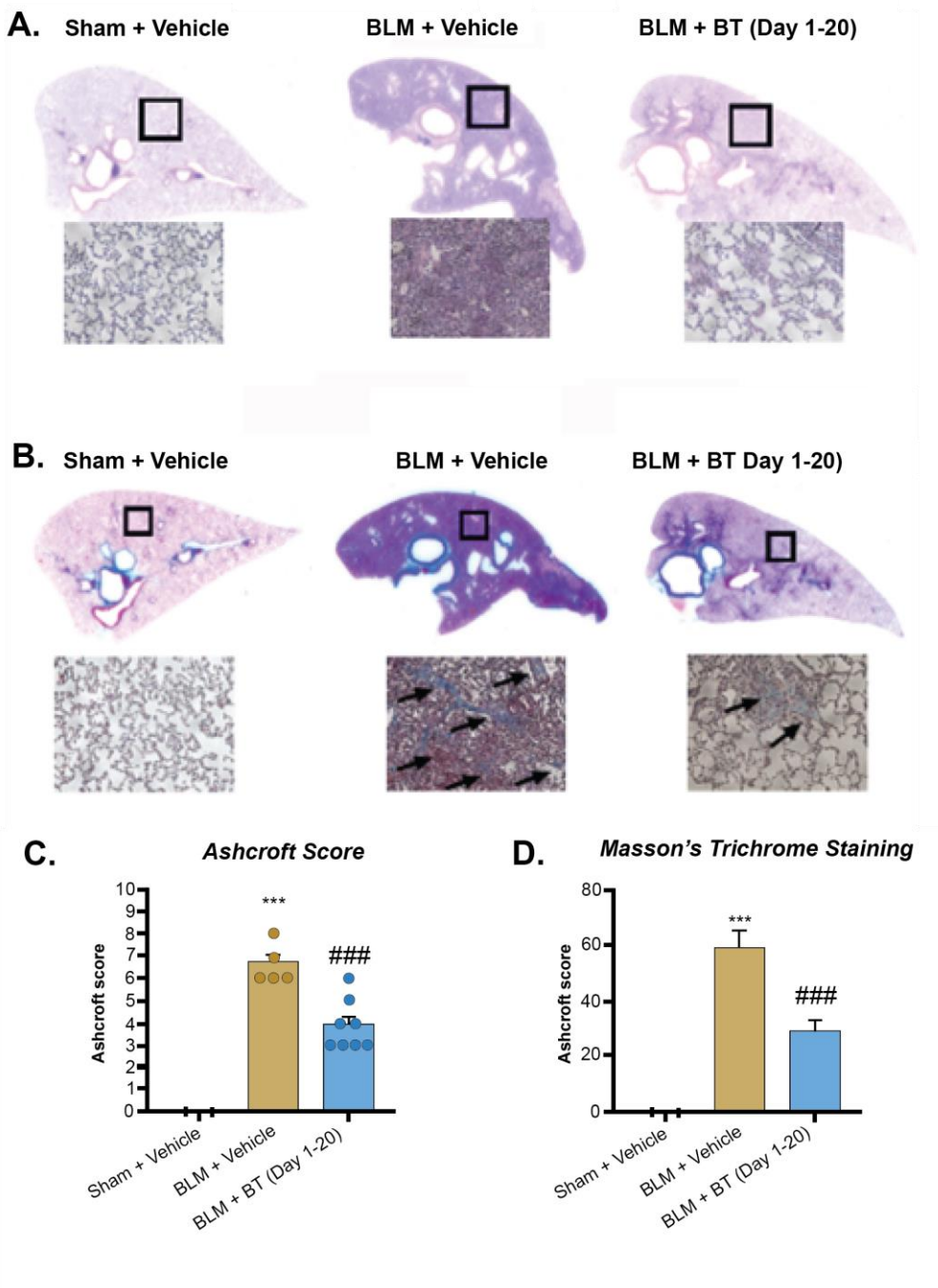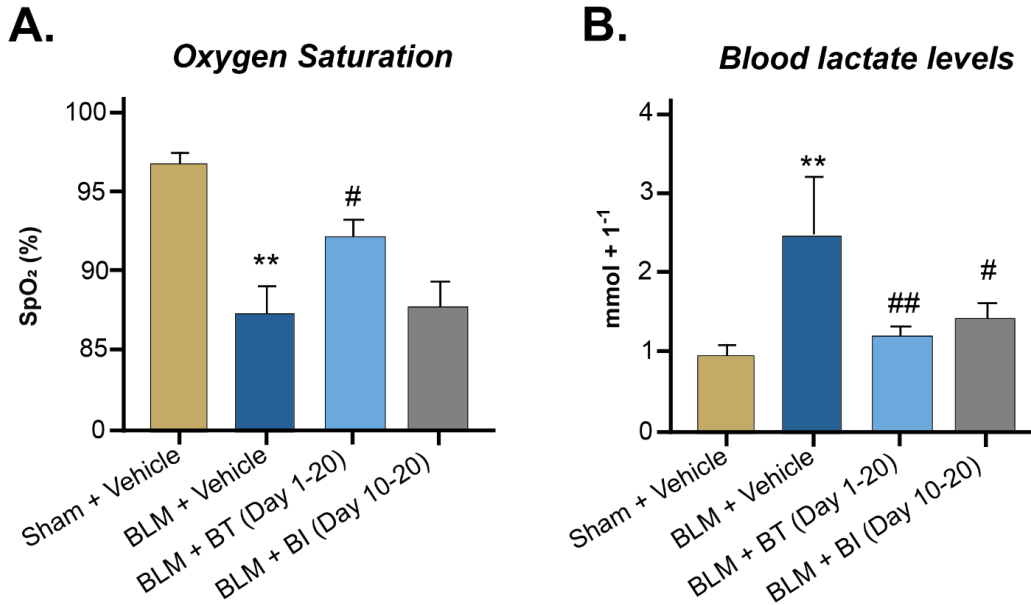

BALF: Bronchoalveolar lavage; BLM: Bleomycin; Sham: Non-induced animals with the vehicle.
BT: Brilaroxazine treatment Days 1-20; BI: Brilaroxazine treatment Days 10-20.
*** $P<0.001$; as compared to Sham.
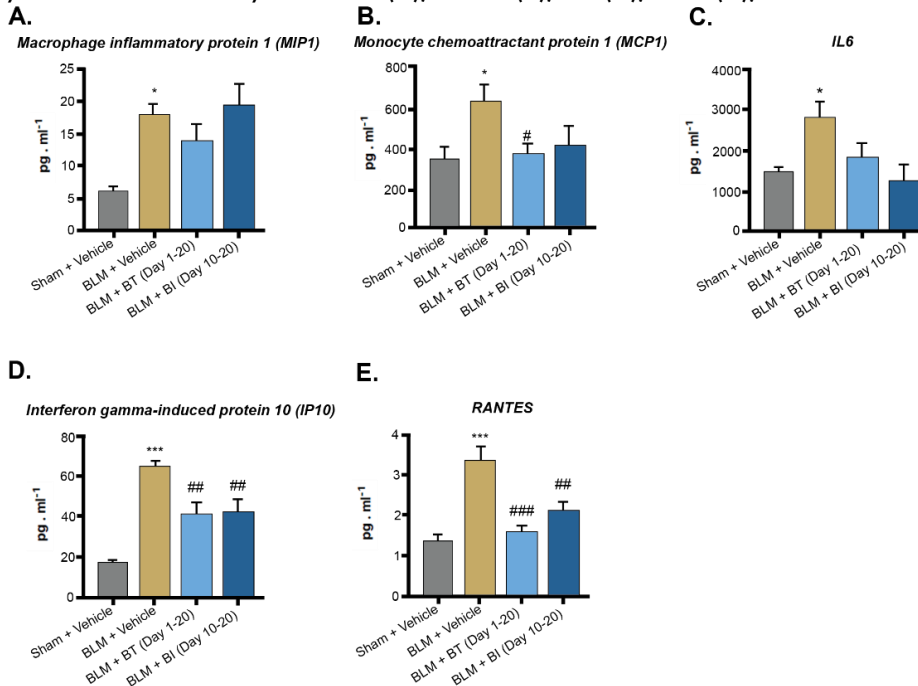### $P<0.001$; as compared to BLM+Veh.

Fig. 7. BLM-induced effects on cardiopulmonary capacity, blood oxygen saturation (A) and blood lactate levels (B) measured at Day 21

BALF: Bronchoalveolar lavage; BLM: Bleomycin; Sham: Non-induced animals with the vehicle.
BT: Brilaroxazine treatment Days 1-20; BI: Brilaroxazine treatment Days 10-20.
** $P<0.01$; as compared to Sham.
# $P<0.05$; as compared to BLM+Veh.
$P<0.01$; as compared to BLM+Veh.

Fig. 8. BALF cytokines levels on Day 21: MIP1 (A); MCP1 (B); IL6 (C); IP10 (D); and RANTES (E).

BALF: Bronchoalveolar lavage; BLM: Bleomycin; Sham: Non-induced animals with the vehicle.
BT: Brilaroxazine treatment Days 1-20; BI: Brilaroxazine treatment Days 10-20.
* $P<0.05$; as compared to Sham.
*** $P<0.001$; as compared to Sham.
# $P<0.05$; as compared to BLM+Veh.
$P<0.01$; as compared to BLM+Veh.
$P<0.001$; as compared to BLM+Veh

The development of pulmonary fibrosis involves a complex interaction between multiple cells and molecules. In IPF, the invasion and dysregulation of fibroblasts play a vital role in the transformation of the lung tissue[31,32]. The increased proliferation, along with the decreased apoptosis, of these cells results in an increased number of fibroblasts converting to extracellular matrix (ECM)-producing mesenchymal cells, activated fibroblasts, leading to an over-accumulation of fibrotic tissue in the lungs[33]. After lung injury, epithelial cells release inflammatory mediators, initiating an antifibrinolytic coagulation cascade and subsequent leukocyte (e.g., neutrophils, T cells, and macrophages) recruitment[34]. Furthermore, inflammatory cells also play a crucial role in the pathogenesis of pulmonary fibrosis by producing fibrogenic cytokines (e.g., MIP-1, MCP-1, IL-6, IP-10, and RANTES) to create and maintain a profibrotic microenvironment. These molecules modulate chemotaxis, proliferation, and cytokine expression in leucocyte subsets. The inflammatory cells express MCP-1 and MIP-1, both of which contribute to the initiation and maintenance of the bleomycin-induced pulmonary lesion. IL-6, secreted by activated T lymphocytes, is also fibrogenic and contributes to fibroblast proliferation and differentiation. IP-10 is a chemoattractant for activated T cells. Finally, RANTES is chemotactic for T cells, eosinophils, and basophils. It plays an active role in recruiting leukocytes into inflammatory sites. Enhanced levels of these cytokines in the lungs are present in pulmonary fibrosis.

Observations from preclinical work suggest that brilaroxazine could exert its antifibrotic effect via an anti-inflammatory mechanism. This study showed that the levels of MIP-1, MCP-1, IL-6, IP-10, and RANTES significantly increased in the BALF of the BLM animals. These findings suggest both an inflammatory and profibrotic role of these different cytokines/chemokines. Moreover, BT significantly reduced the production of MCP-1, IP-10, and RANTES and with a trend for MIP-1 and IL-6 in BALF. BI significantly lowered the production of IP-10 and RANTES.

Study results suggest that brilaroxazine may possess both anti-inflammatory and anti-fibrotic effects. Concerning an antifibrotic impact, the study evaluated the amount of hydroxyproline, the predominant amino acid component of collagen. It also quantified the fibrosis content by Masson's trichrome staining by histology, such as the morphology changes by H&E staining. The ability of brilaroxazine to inhibit BLM-induced up-regulation of hydroxyproline content and fibrosis further support the antifibrotic role of brilaroxazine in pul

monary fibrosis. Interestingly, differences with the non-treated induced and BI groups were more significant than differences between this control group and BT groups ($P<.01$, $P<0.5$ respectively, BLM). This finding might suggest that intervention by BI might exert more of an anti-fibrotic effect, whereas treatment/prevention by BT might involve both anti-inflammatory and anti-fibrotic effects.

The Rationale for 5-HT in IPF

5-HT receptor signaling plays a crucial role in IPF development and pathobiology[35,36]. Through its powerful vasoactive effects, serotonin can stimulate the proliferation and fibrogenic actions of lung fibroblasts. Serotonin signaling produces a powerful vasoactive effect on the pulmonary arteries and stimulates inflammation, proliferation and fibrogenic actions of lung myofibroblasts, the principal effector cells responsible for ECM deposition[15]. SERT facilitates 5-HT uptake by platelets and mast cells, which transport 5-HT to tissues[15]. In the respiratory system pathologies involving endothelial or epithelial damage, it is these platelets, endothelial cells, and mast cells that become activated at sites of vascular injury. The release of 5-HT by these cells increases the local 5-HT concentration, and 5-HT_2 receptor's downstream signaling cascades subsequently facilitate the release of transforming growth factor beta (TGF-β)[1,15,36]. In binding to the 5-HT_2 receptors on resident fibroblasts, 5-HT facilitates the progression of myofibroblast differentiation, increased ECM deposition, and fibrotic remodeling[36].

Ultimately, bronchoconstriction, pulmonary arterial constriction, and stimulation of hypertrophic and hyperplastic alterations in myofibroblasts and smooth muscle cells occur[15]. Therefore, 5-HT plays a fundamental functional and mechanistic role in the pulmonary vasculature. It also acts in 5HT-signaling pathways and receptors in vasomotor and proliferative actions of vascular endothelial and smooth muscle cells of the lungs.

An accumulating body of evidence suggests that 5-$HT_{2B/7}$ receptor antagonists to act both as vasodilators and as inhibitors of vascular fibrosis and pro-inflammatory cytokines (e.g., tumor necrosis factor-alpha [TNF-α], TGF-β, and interleukin-1 beta [IL-1β], and IL-6)[10,15,35]. It is, therefore, hypothesized that serotonin-receptor-pathway-modulating agents might serve as potential treatments for IPF.

These observations have been consistent with the

potential effect of a 5-HT$_{2B}$ receptor antagonist. A study in IPF patients identified the increased expression of 5-HT$_{2B}$ receptor exists in the lungs, mainly in the epithelium[17]. Moreover, terugide (a 5-HT$_{2B}$ receptor antagonist) improved lung functions and decreased fibrosis, confirming earlier observations that BLM-IPF was associated with increased 5-HT in lungs and attenuated with a 5-HT$_{2B}$ receptor antagonist[19,20]. In light of these observations, brilaroxazine by its potently selective 5-HT$_{2B/7}$ antagonistic activities represents a potential IPF treatment option to evaluate.

Areas for Further Research with Brilaroxazine

The primary focus of this study was to assess the effect of brilaroxazine on IPF utilizing the standard BLM model in rats. As anticipated, brilaroxazine demonstrated robust impact on reduction of the pulmonary fibrosis besides improving the vitals and reducing inflammatory cytokines. This work has prompted additional questions of interest with brilaroxazine worthy in future studies.

Most notable would be the influence of brilaroxazine on the mechanical aspects of IPF. Priority would be to elucidate in more detail, both anti-inflammatory and anti-fibrotic effects of brilaroxazine. Of particular interest would be the compound's effect on profibrotic cytokines, such as TGF-β, fibroblast growth factor receptors (FGF), and platelet-derived growth factor (PDGF). Of additional interest would involve the compound's interaction with not only 5-HT-receptors but also with DA-receptors. Of final interest would be its effect on various cell types, cell-cell interactions (including adhesion) involved with fibrosis and IPF pathology.

Additionally, there is interest in the effects of brilaroxazine in comparison with, and in combination with, nintedanib and pirfenidone, both of which are approved drugs for the treatment of IPF. Mono- and co-administered treatments in BLM IPF in rats are in progress. Results of these studies will be published shortly.

Conclusions

In light of the actual criteria for the demonstration of efficacy for IPF treatment, brilaroxazine was able to significantly affect all important biomarkers and actual endpoints illustrated in the present study. Treatment with brilaroxazine attenuated BLM-induced pulmonary fibrosis, inflammation, ECM deposition (collagen) most likely through its 5-HT$_{2B/7}$ receptor antagonist activities and improved cardiac and pulmonary functions in rodents. Brilaroxazine - both as a preventive treatment starting Day 1 (BT) and as interventional therapy (BI) beginning on Day 10 following BLM induction reduced IPF progression. Positive effects on body weight, survival, lung edema, fibrogenic cytokine production, hydroxyproline content, and respiratory resistance, and cardiopulmonary capacity provide supportive evidence that Brilaroxazine impacts both the functional and pathologic effects associated with IPF. As compared with the BLM, the BT group was significant across a broader array of parameters than those seen in the BI group, which still showed numerical improvements. These functional improvements might be related to the pleiotropic or combined effect of brilaroxazine on the pathological factors contributing to inflammation, fibrosis and its proliferation in the lungs. Furthermore, lower numbers of rats in the BLM group due to mortality and the need to harvest animals on Day 21, may have precluded the ability to see the full impact and statistical significance of BI. Nevertheless, the overall effect is exceptionally encouraging and indicative that brilaroxazine is a potentially efficacious therapy for the treatment of IPF.

Conflicts of Interest

Laxminarayan Bhat, Ph.D., Seema R Bhat, M.Sc., are employees of Reviva Pharmaceuticals Holdings, Inc., Cuprtino, CA, USA

Marie-Claude Nault, DCS, Marzena Biernat, DVM, Ph.D., Sebastien M. Labbe, Ph.D., are employees of IPS Therapeutique, Sherbrooke, Quebec, Canada which received funding from Reviva Pharmaceuticals Holdings, Inc. for this study.

References

1. Nalysnyk L, Cid-Ruzafa J, Rotella P, Esser D. Incidence and prevalence of idiopathic pulmonary fibrosis: review of the literature. *European Respiratory Review*. 2012;21(126):355-361.

2. Moore BB, Lawson WE, Oury TD, Sisson TH, Raghavendran K, Hogaboam CM. Translational Review. *Am J Respir Cell Mol Biol*. 2013;49(2):167-179.

3. Bors M, Tomic R, Perlman DM, Kim HJ, Whelan TPM. Cognitive function in idiopathic pulmonary fibrosis. *Chron Respir Dis*. 2015;12(4):365-372.

4. Hutchinson J, Fogarty A, Hubbard R, McKeever T. Global incidence and mortality of idiopathic pulmonary fibrosis: a systematic review. *European Respiratory Journal*. 2015;46(3):795-806.

5. Puglisi S, Torrisi SE, Vindigni V, et al. New perspectives on management of idiopathic pulmonary fibrosis. *Ther Adv Chronic Dis*. 2016;7(2):108-120.

6. Raghu G, Weycker D, Edelsberg J, Bradford WZ, Oster G. Incidence and prevalence of idiopathic pulmonary fibrosis. *Am J Respir Crit Care Med*. 2006;174(7):810-816.

7. Meltzer EB, Noble PW. Idiopathic pulmonary fibrosis. *Orphanet J Rare Dis*. 2008;3(1):1-15.

8. Sakai N, Tager AM. Fibrosis of two: Epithelial cell-fibroblast interactions in pulmonary fibrosis. *Biochimica et Biophysica Acta (BBA)-Molecular Basis of Disease*. 2013;1832(7):911-921.

9. Raghu G, Rochwerg B, Zhang Y, et al. An official ATS/ERS/JRS/ALAT clinical practice guideline: treatment of idiopathic pulmonary fibrosis. An update of the 2011 clinical practice guideline. *Am J Respir Crit Care Med*. 2015;192(2):e3-e19.

10. Tzouvelekis A, Bonella F, Spagnolo P. Update on therapeutic management of idiopathic pulmonary fibrosis. *Ther Clin Risk Manag*. Published online 2015:359-370.

11. Canestaro WJ, Forrester S, Ho L, Devine B. Drug therapy for treatment of idiopathic pulmonary fibrosis: a systematic review and network meta-analysis. *Value in Health*. 2015;18(3):A170.

12. Walter N, Collard HR, King Jr TE. Current perspectives on the treatment of idiopathic pulmonary fibrosis. *Proc Am Thorac Soc*. 2006;3(4):330-338.

13. ESBRIET® (pirfenidone) capsules, for oral use Initial U.S. Approval: 2014. https://www.accessdata.fda.gov/drugsatfda_docs/label/2014/022535s000lbl.pdf. (Accessed 2 February 2018).

14. OFEV® (nintedanib) capsules, for oral use Initial U.S. Approval: 2014 https://www.accessdata.fda.gov/drugsatfda_docs/label/2014/205832s000lbl.pdf. Accessed February 16, 2018.

15. Mann DA, Oakley F. Serotonin paracrine signaling in tissue fibrosis. *Biochimica et Biophysica Acta (BBA)-Molecular Basis of Disease*. 2013;1832(7):905-910.

16. Dees C, Akhmetshina A, Zerr P, et al. Platelet-derived serotonin links vascular disease and tissue fibrosis. *Journal of Experimental Medicine*. 2011;208(5):961-972.

17. Königshoff M, Dumitrascu R, Udalov S, et al. Increased expression of 5-hydroxytryptamine2A/B receptors in idiopathic pulmonary fibrosis: a rationale for therapeutic intervention. *Thorax*. 2010;65(11):949-955.

18. Pan J, Copland I, Post M, Yeger H, Cutz E. Mechanical stretch-induced serotonin release from pulmonary neuroendocrine cells: implications for lung development. *American Journal of Physiology-Lung Cellular and Molecular Physiology*. 2006;290(1):L185-L193.

19. Dumitrascu R, Kulcke C, Königshoff M, et al. Terguride ameliorates monocrotaline-induced pulmonary hypertension in rats. *European Respiratory Journal*. 2011;37(5):1104-1118.

20. Fabre A, Marchal-Somme J, Marchand-Adam S, et al. Modulation of bleomycin-induced lung fibrosis by serotonin receptor antagonists in mice. *European Respiratory Journal*. 2008;32(2):426-436.

21. Tawfik MK, Makary S. 5-HT7 receptor antagonism (SB-269970) attenuates bleomycin-induced pulmonary fibrosis in rats via downregulating oxidative burden and inflammatory cascades and ameliorating collagen deposition: comparison to terguride. *Eur J Pharmacol*. 2017;814:114-123.

22. Bhat L, Hawkinson J, Cantillon M, et al. RP5063, a novel, multimodal, serotonin receptor modulator, prevents monocrotaline-induced pulmonary arterial hypertension in rats. *Eur J Pharmacol*. 2017;810:92-99.

23. Cantillon M, Prakash A, Alexander A, Ings R, Sweitzer D, Bhat L. Dopamine Serotonin Stabilizer RP5063: A Randomized, Double-blind, Placebo-controlled Multicenter Trial of Safety and Efficacy in Exacerbation of Schizophrenia or Schizoaffective Disorder. *Schizophr Res*. 2017;189:126-133. doi:10.1016/j.schres.2017.01.043.

24. Köster LS, Carbon M, Correll CU. Emerging drugs for schizophrenia: an update. *Expert Opin Emerg Drugs*. 2014;19(4):511-531.

25. Cantillon M, Ings R, Bhat L. Initial Clinical Experience of RP5063 following single doses in normal healthy volunteers and multiple doses in patients with stable schizophrenia. *Clin Transl Sci*. 2018;11(4):387-396.

26. Cantillon M, Ings R, Bhat L. Pharmacokinetics of RP5063 following single doses to normal healthy volunteers and multiple doses over 10 days to stable schizophrenic patients. *Clin Transl Sci*. 2018;11(4):378-386.

27. Bhat L, Hawkinson J, Cantillon M, et al. RP5063, a novel, multimodal, serotonin receptor modulator, prevents Sugen 5416-hypoxia–induced pulmonary arterial hypertension in rats. *Eur J Pharmacol*. 2017;810:83-91.

28. Bhat L, Hawkinson J, Cantillon M, et al. Evaluation of the effects of RP5063, a novel, multimodal, serotonin receptor modulator, as single-agent therapy and co-administrated with sildenafil, bosentan, and treprostinil in a monocrotaline-induced pulmonary arterial hypertension rat model. *Eur J Pharmacol*. 2018;827:159-166.

29. Liu Y, Lu F, Kang L, Wang Z, Wang Y. Pirfenidone attenuates bleomycin-induced pulmonary fibrosis in mice by regulating Nrf2/Bach1 equilibrium. *BMC Pulm Med*. 2017;17:1-11.

30. Moeller A, Ask K, Warburton D, Gauldie J, Kolb M. The bleomycin animal model: a useful tool to investigate treatment options for idiopathic pulmonary fibrosis? *Int J Biochem Cell Biol*. 2008;40(3):362-382.

31. Calado RT. Telomeres in lung diseases. *Prog Mol Biol Transl Sci*. 2014;125:173-183.

32. Lovgren AK, Kovacs JJ, Xie T, et al. β-arrestin deficiency protects against pulmonary fibrosis in mice and prevents fibroblast invasion of extracellular matrix. *Sci Transl Med*. 2011;3(74):74ra23-74ra23.

33. Travis WD, Costabel U, Hansell DM, et al. An official American Thoracic Society/European Respiratory Society statement: update of the international multidisciplinary classification of the idiopathic interstitial pneumonias. *Am J Respir Crit Care Med*. 2013;188(6):733-748.

34. Todd NW, Luzina IG, Atamas SP. Molecular and cellular mechanisms of pulmonary fibrosis. *Fibrogenesis Tissue Repair*. 2012;5(1):1-24.

35. Wynn TA. Integrating mechanisms of pulmonary fibrosis. *Journal of Experimental Medicine*. 2011;208(7):1339-1350.

36. Löfdahl A, Rydell-Törmänen K, Müller C, et al. 5-HT 2B receptor antagonists attenuate myofibroblast differentiation and subsequent fibrotic responses in vitro and in vivo. *Physiol Rep*. 2016;4(15):e12873.